WORLD JOURNAL OF PHARMACEUTICAL RESEARCH
SJIF Impact Factor 6.805
Volume 5, Issue 3, 1778-1792. Research Article ISSN 2277– 7105

MOLECULAR INTERACTIONS OF NICOTINE AND THE NITROGENOUS BASES OF DNA AND RNA CALCULATED BY IMPROVED QUANTUM METHODS

M. González-Pérez*, M. Briteño-Vázquez, F. A. García-Barrera, A. K. Ham-Tirado, J.M. López-Oglesby, M.R. Salazar-Amador and P.F. Pacheco-García.

Graduate Department of Biomedical Engineering, Universidad Popular Autónoma del Estado de Puebla (UPAEP), 72410, México.

Article Received on
18 Jan 2016,

Revised on 09 Feb 2016,
Accepted on 01 March 2016

***Correspondence for Author**
Dr. M. González-Pérez
Graduate Department of Biomedical Engineering, Universidad Popular Autónoma del Estado de Puebla (UPAEP), 72410, México.

ABSTRACT

Nicotine (Nic o N) has caused much damage to humans. Exposure to Nic during the development stage of the fetus can lead to several disorders. The objective of this work was to calculate all possible interactions of Nic vs. Nitrogen Bases (NB) for DNA and RNA using Semi-Empirical Parameterized Method 3 (SE-PM3). These calculations were performed using the molecular simulator Hyper Chem (HC). The improved calculations were based on the novel Electron Transfer Coefficient (ETC) theory posited by the authors in previous work. This theory is the calculus of the ratio of dividing Band Gap (BG) / Electrostatic Potential (EP). This ratio indicates the number of multiples of its EP that the electron needs to jump its BG. As the result, we calculated 36 Interactions Cross Band (ICB) of NB and 13 ICB of Nic vs. NB. We conclude that N can be confused with the A in the genesis of RNA because the similar value of ETC (24.092 and 24.240) for the pairs pair A:U and N:U. It is noted that the N gives an electron cloud in the same way that A does.

KEYWORDS: Nicotine, Nitrogenous bases, DNA and RNA, Quantum methods, SE-PM3

I. INTRODUCTION

a. The harm caused by Nic

Nic has caused much damage to humans. Many studies show that Nic may affect pluripotent cell differentiation in fibroblasts and, in particular, the differentiation of embryonic stem cells.[1] The reduced fertility and increased follicular atresia in animals exposed to Nic may

be due to disruption of the regulation of Insulin Growth Factor (IGF). In the ovaries, and uterus and lactational exposure to Nic alters the intra-ovarian IGF system in adult female rats.[2, 37]

The consumption of snuff in human pregnancy increases the risk of complications for both mother and fetus. In macaque's pregnancy, this Nic exposure decreases lung function though maternal vitamin C supplementation attenuates these detrimental effects.[3] Nic affects uterus histology and the oviduct while melatonin administration reduces this damage.[4]

Other results obtained by researchers are that the sub-acute exposure to Nic has an effect on cerebral microvascular thrombosis and systemic toxicity in mice.[5] Another result was the evaluation of the impact of chronic administration of Nic in bone mineral homeostasis in the growth of young rats. Compared to the effects on adult male rats, this exposure induces bone changes that vary with age.[6]

Furthermore, the concentrations of Nic smoking (100 -300 nm) interfere with cholinergic signaling in the prefrontal cortex of mice.[7] The study of cholinergic receptor systems and has generated great interest. It is because various changes in cholinergic transmission have been related, directly or indirectly, with severe disorders such as Alzheimer's and Parkinson.[8] The results of exposure to Nic in the development stage can also lead to neurobehavioral disorders. The clinical relevance of these studies is a justification for insisting that all people in general and the youth group be particularly risky. It should be warned of the risks of adverse effects of Nic on the biological system as a whole.[9]

In this article, we study the molecular interactions of Nic and the nitrogenous bases of DNA and RNA by quantum computational methods.

b. Uracil and nitrogenous base pairs

Researchers have studied the Uracil (U) for many years. These studies range from its conversion from cytosine until it generates mispair with other bases.[10-13]

The deamination of cytosine generates the purine base U. U produces the mispair mating G:U.[14] It is removed from DNA by the U of DNA glycosylase enzyme (UDG).[15-16, 36, 39] UDG is specific for U.[17-18]

For example, the pair T:X emerges through misincorporation during DNA replication.[18] In a particular case, the mispair T:G is much easier to synthesize than couples allowed T:A and C:G.[19]

Other combinations of the base were studied and found that misalignments base pair Purine-Purine can form a variety of configurations. These settings depend on solution conditions. The pairs G:G were identified by X-ray diffractograms and nuclear magnetic resonance (NMR). These devices can view settings anti-pair and syn G:G.[20] Seeking, these combinations, it was suggested that the measurement of the magnetic properties of DNA could be a direct path to detect the mispair G:A.[21] This mechanism of recognition stems from the lack of verification for the pair G: that particular conformations adopted.[22]

c. Quantum computational methodology

Computational methods are imperative in predicting chemical and biochemical reactions. These methods can save time, materials and reagents in laboratory experiments.

The principles of Quantitative Structure-Activity Relationship (QSAR) could spread to enrich physicochemical structural indices. The molecular fragments or structural designs (or other molecular residues) provide detailed maps of the biological chemical interactions.[23] The surfaces of the interaction of DNA[38] and proteins can be identified with computational support.[24-25] The theoretical vibrational frequencies and geometric parameters (bond lengths and bond angles) can be calculated using ab initio Hartree-Fock (HF).[26]

Computational-based quantum chemistry methods also identify more stable molecular systems tautomers for which the common chemical knowledge is not enough to make definitive predictions.[27]

Researchers extended the protocol to simulate a computational spectroscopic property of a solid molecular U and effects of the hydrogen bonds in the IR spectrum.[28] Hydrogenation enthalpy of U was determined and found that U has 30.0% of the aromatic character in the gas phase.[29] It was studied experimentally, and the results were compared to three quantum computations methylated U, in particular, 5,6-dimethyl, 1, 3, 5-trimethyl- and 1, 3, 5, 6 - tetramethyl. The comparison results were excellent.[30] Methods of density functional theory plane wave are used to explore ways and configurations adsorption molecules U on a gold surface.[31]

For this work, we explored the molecular interactions of Nic and the nitrogenous bases of DNA and RNA by the quantum method SE-PM3.

II. METHODOLOGY

a. Abbreviations

Highest Occupied Molecular Orbital (HOMO). Lowest Unoccupied Molecular Orbital (LUMO). Band Gap (BG), Negative Energy (E-). Positive Energy (E+). Electrostatic Potential (EP). Electronic Transfer Coefficient (ETC). Uracil Tautomer 1 (U1). Uracil Tautomer 2 (U2) figure 1.

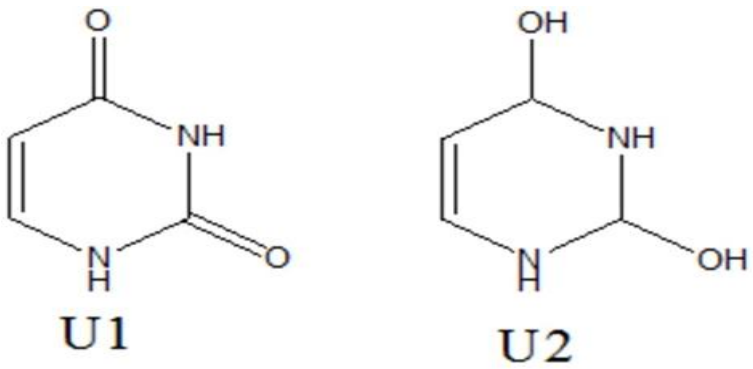

FIG. 1. Tautomers of U. U tautomer U1 has ketone links. U tautomer U2 has hydroxyl links.

b. Computational Methods

The simulations were performed with molecular simulator Hyper Chem (HC). (Hyper Chem. Hypercube, MultiON for Windows. Serial #12-800-1501800080. MultiON. Insurgentes Sur 1236 - 301 Tlacoquemecatl Col. del Valle, Delegación Benito Juárez, D. F., México CP. 03200).

The computational model was; HC Semi-Empirical Parameterized Model number 3 (SE-PM3) to draw the corresponding molecules. These were then processed using SE-PM3. The geometry was optimized with the Polak Ribiere method. The computational quantum chemistry variables were then calculated: HOMO-LUMO, BG, EP and other properties, resulting in a Tab-delimited Table for BG and EP.

The specific parameters selected for each of the simulations were as follows: SET UP. Semi-Empirical Method: PM3. Semi-Empirical Options: Charge and Spin. Total Charge 0. Spin Multiplicity 1. SCF Control. Converge limit 0.01. Interaction limit 1000. Accelerate converge

Yes. Spin Pairing Lowest. Overlap Weighting Factors Sigma-Sigma 1, Pi-Pi 1. Polarizabilities do not calculate.

Computation 1. Geometry Optimization. Algorithm Polak Ribiere (conjugate gradient). Options Termination conditions. RMS gradient of 0.1 kcal/mol or 1000 maximum cycles. In vacuo yes. Screen refresh period one cycles.

Computation 2. Orbitals. Plot Orbital Options Isosurface Rendering. Orbital Contour Value 0.05. Rendering Wire meshes Isosurface Grid. Grid meshes size Coarse. Grid layout Default. Gird contour Default. Transparency level Default.

Computation 3. Plot Molecular Graphs. Plot Molecular Options. Molecular Properties. Properties. Electrostatic Potential Yes. Representations. 3D Mapped Isosurface. Grid Mesh Size Coarse. Grid layout Default. Contour gird Default. Isosurface Rereading. Total Charge Density Contour Value (TCDCV) 0.015. Rendering Wire mesh. Transparency level Default. Mapped Options Functions Default.

c. Formulas

The calculations were based on ETC theory.[32] This theory is calculating the ratio of dividing the BG / EP. This ratio indicates the multiples of the EP that the electron jumps its BG.

$$ETC = \left|\frac{BG}{EP}\right| \quad (1)$$

The EP is equal to the absolute value of the difference (E+) – (E-).

$$EP = |E_+ - E_-| \quad (2)$$

The BG is equal to the absolute value of the difference (HOMO) – (LUMO)[32-34] (Perez, 2014; Gonzalez-Perez, 2015).

$$BG = |HOMO - LUMO| \quad (3)$$

III. RESULT AND DISCUSSION

Table I shows the electronic interactions between molecules of the same chemical species sorted by ETC column. This order indicates the stability of substances. The interaction I is the most stable, and interaction VII is the least stable (Figure 2).

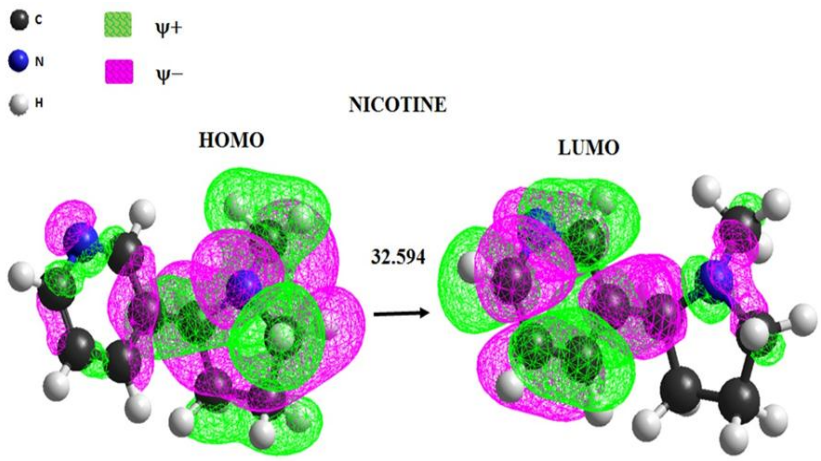

FIG. 2. This figure shows the interaction between two molecules of Nic. The electrons flow from HOMO located in the ring of five atoms to the LUMO situated in the ring of six atoms. It is the most unstable or more reactive of all substances are shown in Table I.

The reactivity is in the opposite direction. From the least to ETC = 32.594 are the highest among all substances in Table I. This interaction VII belongs to the Nic. Therefore, the order of the ETCs indicates that the Nic attacks anyone of nitrogenous bases.

Table I. Electronic interactions between molecules of the same chemical species.

Interaction number	Gives Electron cloud	Get Electron cloud	HOMO (eV)	LUMO (eV)	BG (eV)	E- (eV/a^0)	E+ (eV/a^0)	EP (eV/a^0)	ETC [a]
I	G	G	-8.537	-0.206	8.331	-0.150	0.172	0.322	25.872
II	C	C	-9.142	-0.344	8.799	-0.174	0.161	0.335	26.265
III	U2	U2	-9.910	-0.415	9.495	-0.147	0.202	0.349	27.208
IV	A	A	-8.654	-0.213	8.441	-0.140	0.156	0.296	28.518
V	T	T	-9.441	-0.475	8.966	-0.123	0.169	0.292	30.707
VI	U1	U1	-9.710	-0.511	9.200	-0.126	0.171	0.297	30.975
VII	**Nic**	**Nic**	**-9.190**	**0.100**	**9.289**	0.125	**-0.160**	**0.285**	**32.594**

[a] The ETC is considered dimensionless. Energy unit is the electron volt (eV).

The unit of Electrostatic Potential is (electron - volt) / Angstroms.

Table II shows the interactions of cross-bands of the nitrogenous bases. It is sorted by the ETC values (last column). It was according to the Lane prediction.[20]

Table II. Electronic interactions between molecules nitrogenized bases. Cross band.

Interaction number	Gives [a] electron cloud	Get [b] electron cloud	HOMO	LUMO	BG	E-	E+	EP	ETC
1	G	U2	-8.537	-0.415	8.122	-0.150	0.202	0.352	23.074
2	C	U2	-9.142	-0.415	8.728	-0.174	0.202	0.376	23.212
3	A	U2	-8.654	-0.415	8.240	-0.140	0.202	0.342	24.092
4	G	U1	-8.537	-0.511	8.026	-0.150	0.171	0.321	25.003
5	C	U1	-9.142	-0.511	8.632	-0.174	0.171	0.345	25.019
6	C	T	-9.142	-0.475	8.668	-0.174	0.169	0.343	25.270
7	G	T	-8.537	-0.475	8.062	-0.150	0.169	0.319	25.273
8	C	G	-9.142	-0.206	8.936	-0.174	0.172	0.346	25.827
9	G	G	-8.537	-0.206	8.331	-0.150	0.172	0.322	25.872
10	A	U1	-8.654	-0.511	8.144	-0.140	0.171	0.311	26.185
11	C	C	-9.142	-0.344	8.799	-0.174	0.161	0.335	26.265
12	G	C	-8.537	-0.344	8.193	-0.150	0.161	0.311	26.345
13	A	T	-8.654	-0.475	8.180	-0.140	0.169	0.309	26.471
14	C	A	-9.142	-0.213	8.929	-0.174	0.156	0.330	27.058
15	A	G	-8.654	-0.206	8.448	-0.140	0.172	0.312	27.078
16	G	A	-8.537	-0.213	8.324	-0.150	0.156	0.306	27.202
17	U2	U2	-9.910	-0.415	9.495	-0.147	0.202	0.349	27.208
18	A	C	-8.654	-0.344	8.311	-0.140	0.161	0.301	27.610
19	T	U2	-9.441	-0.415	9.026	-0.123	0.202	0.325	27.773
20	U1	U2	-9.710	-0.415	9.296	-0.126	0.202	0.328	28.340
21	A	A	-8.654	-0.213	8.441	-0.140	0.156	0.296	28.518
22	U2	U1	-9.910	-0.511	9.399	-0.147	0.171	0.318	29.558
23	U2	T	-9.910	-0.475	9.435	-0.147	0.169	0.316	29.859
24	T	U1	-9.441	-0.511	8.930	-0.123	0.171	0.294	30.375
25	U2	G	-9.910	-0.206	9.704	-0.147	0.172	0.319	30.420
26	T	T	-9.441	-0.475	8.966	-0.123	0.169	0.292	30.707
27	U1	U1	-9.710	-0.511	9.200	-0.126	0.171	0.297	30.975
28	U2	C	-9.910	-0.344	9.567	-0.147	0.161	0.308	31.061
29	T	G	-9.441	-0.206	9.235	-0.123	0.172	0.295	31.305
30	U1	T	-9.710	-0.475	9.236	-0.126	0.169	0.295	31.307
31	U1	G	-9.710	-0.206	9.504	-0.126	0.172	0.298	31.894
32	U2	A	-9.910	-0.213	9.697	-0.147	0.156	0.303	32.004
33	T	C	-9.441	-0.344	9.098	-0.123	0.161	0.284	32.033
34	U1	C	-9.710	-0.344	9.367	-0.126	0.161	0.287	32.637
35	T	A	-9.441	-0.213	9.228	-0.123	0.156	0.279	33.076
36	U1	A	-9.710	-0.213	9.497	-0.126	0.156	0.282	33.679

[a]These substances are reducing agents because they are oxidized.

[b]These substances are oxidizing agents because they are reduced.

This table includes Table I (Does not include Nic:Nic).

The lower ETC = 23.047 belong to the interaction G:U2. This interaction is a mispair occurring DNA or RNA. G:U1 or G:U2. These Mispairs are removed from DNA by uracil-DNA glycosylase (UDG).[15, 16, 35] UDG is highly specific for U and shows no activity towards any other base.[14, 35] Specifics for U and shows no activity towards any other base.[14,35]

The biggest ETC = 33.679 belongs to the interaction, U1:A, and not presented naturally to the DNA or RNA.

In general, the base pair partner of the U is not recognized, and the enzyme also acts on A:U base pairs that arise through misincorporation during DNA replication.[17, 35] Furthermore, we can speculate that the small differences between the bases ETCs indicate that the probability of unwanted combined pairs of both DNA and RNA are high. Therefore, mutations are very likely in different directions of flow of electrons.

Table III shows the possible "allowed interactions" between the nitrogenous bases in DNA and RNA. The difference between ETCs interactions cross bands is minuscule. This observation leads us to believe that any of them occurs easily and reaffirms the formation of hydrogen bond of low energy.

The ETC = 24.092 corresponding to the interaction A:U2 is the lowest of the table. This lowest ETC means that is the most likely to occur under these conditions.

Table III. The possible wanted to combine pairs interactions between the nitrogenous bases in DNA and RNA.

Interaction number	Gives Electron cloud	Get electron Cloud	HOMO	LUMO	BG	E-	E+	EP	ETC
3	A	U2	-8.654	-0.415	8.240	-0.140	0.202	0.342	24.092
8	C	G	-9.142	-0.206	8.936	-0.174	0.172	0.346	25.827
10	A	U1	-8.654	-0.511	8.144	-0.140	0.171	0.311	26.185
12	G	C	-8.537	-0.344	8.193	-0.150	0.161	0.311	26.345
13	A	T	-8.654	-0.475	8.180	-0.140	0.169	0.309	26.471
32	U2	A	-9.910	-0.213	9.697	-0.147	0.156	0.303	32.004
35	T	A	-9.441	-0.213	9.228	-0.123	0.156	0.279	33.076
36	U1	A	-9.710	-0.213	9.497	-0.126	0.156	0.282	33.679

This table was extracted from Table II.

Table IV shows the lowest energy interactions of the four hydrogen bonds of the nitrogenous bases in DNA and RNA. The difference between the highest and the lowest value for the

ETCs in Table 4 is 2.38; this means that any one of them is given with relative ease. The interactions 3, 10 and 13 show the best affinity of the A for the U2 and U1 than the T.

Table IV. The lowest energy interactions of the four hydrogen bonds of the nitrogenous bases in DNA and RNA.

No.	Reduction Agent	Oxidant Agent	ETC
3[b]	A	U2	24.09
8[a]	C	G	25.83
10[b]	A	U1	26.19
13[a]	A	T	26.47

[a] The Interactions of lower energy (more stable) for the DNA.

[b] The Interactions of less energy (more stable) for the RNA.

This table was extracted from Table III.

Table V shows the interactions of Nic with nitrogenous bases in cross bands. The ETC = 24.09 (Table IV.A:U2) and ETC = 24.240 of (Table V. N:U2) are nearly equal. This comparison indicates that the Nic competes with A by U2 (figure 3). This competition allows Nic can be confused with the A. The probability of that this confusion causes a mutation, is very high.

The ETC 26.19, (Table IV.A:U2) and ETCs 26.220, 26,489 (Table V. N:U1, N:T) are similar and can also cause confusion.

Table V. Interactions of N with nitrogenous bases in cross bands

Interaction Number	Gives electron cloud	Get electron cloud	HOMO	LUMO	BG	E-	E+	EP	ETC
1	N	U2	-9.190	-0.415	8.775	-0.160	0.202	0.362	24.240
2	N	U1	-9.190	-0.511	8.679	-0.160	0.171	0.331	26.220
3	N	T	-9.190	-0.475	8.715	-0.160	0.169	0.329	26.489
4	N	G	-9.190	-0.206	8.983	-0.160	0.172	0.332	27.058
5	N	C	-9.190	-0.344	8.846	-0.160	0.161	0.321	27.557
6	N	A	-9.190	-0.213	8.976	-0.160	0.156	0.316	28.407
7	C	N	-9.142	0.100	9.242	-0.174	0.125	0.299	30.910
8	G	N	-8.537	0.100	8.637	-0.150	0.125	0.275	31.406
9	N	N	-9.190	0.100	9.289	-0.160	0.125	0.285	32.594
10	A	N	-8.654	0.100	8.754	-0.140	0.125	0.265	33.035
11	U2	N	-9.910	0.100	10.010	-0.147	0.125	0.272	36.802
12	T	N	-9.441	0.100	9.541	-0.123	0.125	0.248	38.472
13	U1	N	-9.710	0.100	9.810	-0.126	0.125	0.251	39.085

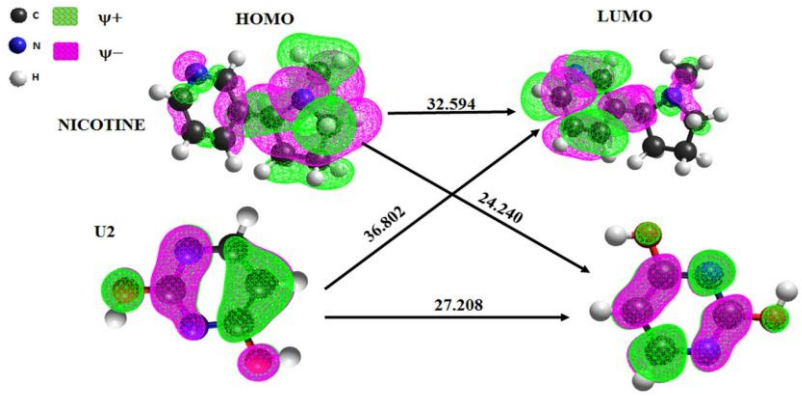

FIG. 3. In this figure the smallest value for all bands of the N interactions with U2 shown (24.240).

This interaction is the most likely path for electron flow.

In general, it can be inferred that Nic can be confused with the A during the genesis of RNA. It is noted that the Nic gives an electron cloud in the same way as A. This reaffirms the confusion between Nic and A in the genesis of RNA. The same phenomenon is observed in the opposite reaction, *i.e*. when the Nic direction acts as oxidizing agent. The interactions 10, 11, 12 and 13 of Table V confirm this supposition. These interactions are the less likely, by the high ETCs present in each of them. In even more general form, the A may be confused with Nic as reducing agent, and an oxidizing agent, i.e., in both directions (Figure4).

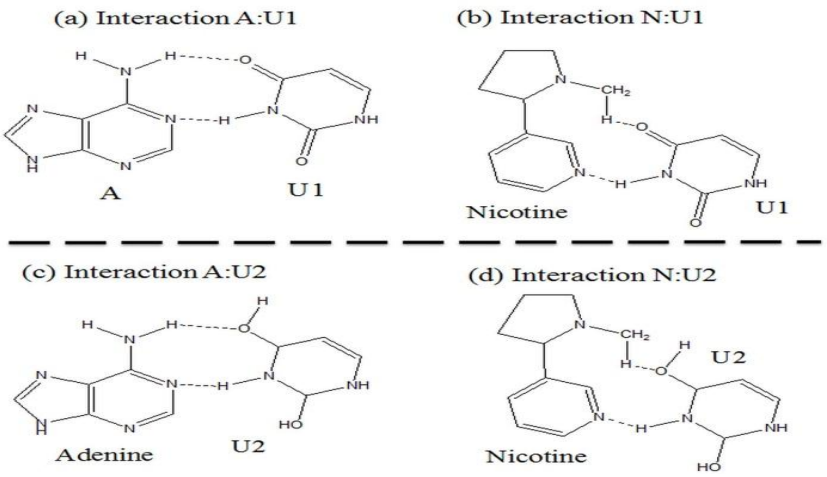

FIG. 4. This figure shows the interactions of the U:A similar to U:Nic.

ETCs difference between (a) and (b) is 0.035.

The ETCs difference between (c) and (d) is 0.148.

The probability of the U forms hydrogen bond with Nic is very high because their cross ETCs have a small difference.

IV. CONCLUSIONS

We calculated the electronic interactions between molecules of the same chemical species of Nitrogen bases or DNA and RNA. The interaction G:G is the most stable (ETC = 25.872) of all (Table I) in concordance with the research by Lane.[20] The interaction Nic:Nic is the least stable (ETC = 32.594). Because of this instability, the interaction Nic:Nic is the highest and, Nic can attack anyone of nitrogenous bases.

We calculated the interactions of cross-bands (36, Table II) of the nitrogenous bases. This calculation was according to with the Lane prediction in 1995.[20] We observed the lower ETC = 23.047 belongs to the interaction G:U2. This interaction is a mispair occurring DNA or RNA.

On the other hand, the interactions in Table IV show the best affinity of the A for the U2 and U1 than the T.

As the principal contribution of this study, it can be inferred that N can be confused with the A in the genesis of RNA. Because the similar value of ETC (24.092 and 24.240) of pair A:U and Nic:U. with Nic giving an electron cloud similarly to A.

The same phenomenon is observed in the opposite reaction when the Nic direction acts as oxidizing agent. The interactions 10, 11, 12 and 13 of Table V confirm this supposition. These interactions are the less likely, by the high ETCs.

In even more general form, the A may be confused by U1 and U2, with Nic as reducing agent, and an oxidizing agent in both directions.

With these findings, another avenue to explain the oncogenic and mutagenic effects of Nic on the human body are proposed in conjunction with the novel ETC method.

REFERENCES

1. Ma, L., Zheng, L. W., Sham, M. H., & Cheung, L. K. Effect of nicotine on gene expression of angiogenic and osteogenic factors in a rabbit model of bone regeneration. Journal or Oral a Maxillofacial Surgery, 2010; 68(4): 777-781.

2. Bruin, J. E., Gerstein, H. C., & Holloway, A. C. Long-term consequences of fetal and neonatal nicotine exposure: a critical review. Toxicological sciences, 2010; 116(2): 364-374.
3. Lo, J., Morgan, T., Roberts, V., Walker, J., Spindel, E., & Frias, A. 50: Vitamin C supplementation mitigates the deleterious effects of chronic nicotine exposure on placental histology in a nonhuman primate model. American Journal of Obstetrics an Gynecology, 2014; 1(210): S33.
4. Seyed Saadat, S. N., Mohammadghasemi, F., Khajeh Jahromi, S., Homafar, M. A., & Haghiri, M. Melatonin protects uterus and oviduct exposed to nicotine in mice. 2014; 7(1): 41-46.
5. Fahim, M. A., Nemmar, A., Al-Salam, S., Dhanasekaram, S., Shafiullah, M., Yasin , J., & Hassan, M. Y. Thromboembolic injury a systemic toxicity induced by nicotine in mice., 2013; 33(3): 345-355.
6. Farag, M. M., Selima, E. A., & Salama, L. A. Impact of chronic nicotine administration on bone mineral content in young and adult rats: A comparative study. European journal of pharmacology, 2013; 720(1): 1-6.
7. Poorthuis, R. B., Bloem, B., Verhoog, M. B., & Mansvelder, H. D. Layer-specific interference with cholinergic signaling in the prefrontal cortex by smoking concentrations of nicotine. The Journal of Neuroscience, 2013; 33(11): 4843-4853.
8. Flores-Soto, ME & Segura-Torres, JE. Structure and function of the acetylcholine of muscarinical and nicotinical type. Rev Mex Neuroci 2005; 6(4): 315-326.
9. Balsevich, G., Poon, A., & Wilking, J. A. The effects of pre-and pos-natal nicotine exposure and genetic background on the striatum and bhavioral phenotypes in mouse. Behavioral Brain Research, 2014; 266: 7-18.
10. Mol CD, Arvai AS, Slupphaug G, Kavli B, Alseth I, et al. Crystal structure and mutational analysis of human uracil-DNA glycosylase: structural basis for specificity and catalysis. Cell, 1995; 80: 869–878.
11. Savva R, McAuley-Hecht K, Brown T, Pearl L. The structural basis of specific base-excision repairs by uracil-DNA glycosylase. Nature, 1995; 373: 487–493.
12. Stivers JT, Pankiewicz KW, Watanabe KA Kinetic mechanism of damage site recognition and uracil flipping by Escherichia coli uracil DNA glycosylase. Biochemistry 1999; 38: 952–963.
13. Imai, K., Slupphaug, G., Lee, W. I., Revy, P., Nonoyama, S., Catalan, N. & Durandy, A. Human uracil–DNA glycosylase deficiency associated with profoundly impaired

immunoglobulin class-switch recombination. Nature Immunology, 2003; 4(10): 1023-1028.

14. Lindahl T An N-glycosidase from Escherichia coli that releases free uracil from DNA containing deaminated cytosine residues. Proc Natl Acad Sci USA 1974; 71: 3649–3653.
15. Krokan HE, Bjoras M Base excision repair. Cold Spring Harb Perspect Biol, 2013; 5: a012583.
16. Friedman JI, Stivers JT Detection of damaged DNA bases by DNA glycosylase enzymes. Biochemistry, 2010; 49: 4957–4967.
17. Tye BK, Nyman PO, Lehman IR, Hochhauser S, Weiss B Transient accumulation of Okazaki fragments as a result of uracil incorporation into nascent DNA. Proc Natl Acad Sci USA 1977; 74: 154–157.
18. Neddermann, P., & Jiricny, J. Efficient removal of uracil from GU mispairs by the mismatch-specific thymine DNA glycosylase from HeLa cells. Proceedings of the National Academy of Sciences, 1994; 91(5): 1642-1646.
19. Imhof, P., & Zahran, M. The effect of a G: T mispair on the dynamics of DNA. PloS one, 2013; 8(1).
20. Lane, A. N., & Peck, B. Conformational flexibility in DNA duplexes containing single G· G mismatches. European Journal of Biochemistry, 1995; 230(3): 1073-1087.
21. Apalkov, V., Berashevich, J., & Chakraborty, T. Unique magnetic signatures of mismatched base pairs in DNA. The Journal of chemical physics, 2010; 132(8): 085102.
22. Berashevich, J., & Chakraborty, T. Thermodynamics of GA mispairs in DNA: Continuum electrostatic model. Journal of Chemical Physics, 2009; 130(1): 15101.
23. Putz, M. V. Residual-QSAR. Implications for genotoxic carcinogenesis. Chem. Cent. J., 2011; 5(111): 22.
24. Roberts, V. A., Pique, M. E., Hsu, S., Li, S., Slupphaug, G., Rambo, R. P. & Woods, V. L. (2012). Combining H/D exchange mass spectroscopy and computational docking reveals extended DNA-binding surface on uracil-DNA glycosylase. Nucleic acids research, gks291.
25. Roberts, V. A., Pique, M. E., Ten Eyck, L. F., & Li, S. Predicting protein–DNA interactions by full search computational docking. Proteins: Structure, Function, and Bioinformatics, 2013; 81(12): 2106-2118.
26. Çırak, Ç., Sert, Y., & Ucun, F. Experimental and computational study on molecular structure and vibrational analysis of a modified biomolecule: 5-bromo-2′-deoxyuridine.

Spectrochimica Acta Part A: Molecular and Biomolecular Spectroscopy, 2012; 92: 406-414.

27. Haranczyk, M., Urbaszek, P., Ng, E. G., & Puzyn, T. Combinatorial× computational× cheminformatics (C3) approach to characterization of congeneric libraries of organic pollutants. Journal of chemical information and modeling, 2012; 52(11): 2902-2909.
28. Fornaro, T., & Biczysko, M. Toward Feasible and Comprehensive Computational Protocol for Simulation of the Spectroscopic Properties of Large Molecular Systems. J. Phys. Chem. A, 2014; 119(21): 5313-5326.
29. Galvão, T. L., Rocha, I. M., Ribeiro da Silva, M. D., & Ribeiro da Silva, M. A. Is Uracil Aromatic? The Enthalpies of Hydrogenation in the Gaseous and Crystalline Phases, and in Aqueous Solution, as Tools to Obtain an Answer. The Journal of Physical Chemistry A, 2013; 117(28): 5826-5836.
30. Notario, R., Emel'Yanenko, V. N., Roux, M. V., Ros, F., Verevkin, S. P., Chickos, J. S., & Liebman, J. F. Thermochemistry of Uracils. Experimental and Computational Enthalpies of Formation of 5, 6-Dimethyl-, 1, 3, 5-Trimethyl-, and 1, 3, 5, 6-Tetramethyluracils. The Journal of Physical Chemistry A, 2012; 117(1): 244-251.
31. Rasheed, T., & Ahmad, S. Computational studies of vibrational spectra and molecular properties of 6-methyluracil using HF, DFT, and MP2 methods. Indian Journal of Physics, 2011; 85(2): 239-260.
32. Perez, M. G., Barrera, F. A. G., Diaz, J. F. M., Torres, M. G., & Oglesby, J. M. L. THEORETICAL CALCULATION OF ELECTRON TRANSFER COEFFICIENT FOR PREDICTING THE FLOW OF ELECTRONS BY PM3, USING 20 AMINO ACIDS, AND NICOTINE. European Scientific Journal, 2014; 10(27).
33. González-Pérez, M. (2015) Applied quantum chemistry. Analysis of the rules of Markovnikov and anti-Markovnikov. International Journal of Science and Advanced Technology. Volume 5 No 5 May.
34. González-Pérez, M. (2015) Methyl chloride vs. Ethyl Chloride. A demonstration of quantum chemical theory by the experimental chemical. Volume 5 No 2 February.
35. Zharkov DO, Mechetin GV, Nevinsky GA Uracil-DNA glycosylase: Structural, thermodynamic and kinetic aspects of lesion search and recognition. Mutat Res, 2010; 685: 11–20.
36. Kimber, S. T., Brown, T., & Fox, K. R. A Mutant of Uracil DNA Glycosylase That Distinguishes between Cytosine and 5-Methylcytosine. PloS one, 2014; 9(4): e95394.

37. Cesta, C. E., Petrik, J. J., Ambraska, H., & Holloway, A. C. In utero and lactational exposure to nicotine alters the intra-ovarian IGF system in adult female rats. Reproductive Biology Insights, 2009; 2, 1.
38. Improta, R., & Barone, V. Excited states behavior of nucleobases in solution: insights from computational studies. In Photoinduced Phenomena in Nucleic Acids. Springer International Publishing, 2015; 1: 329-357.
39. Knævelsrud, I., Slupphaug, G., Leiros, I., Matsuda, A., Ruoff, P., & Bjelland, S. Opposite-base dependent excision of 5-formyluracil from DNA by hSMUG1. International journal of radiation biology, 2009; 85(5): 413-420.